UDC 539.4

Centrifuge Simulation of the Thermal Response of a Dry Sand-Embedded Diaphragm Wall

S. You,[a] C. H. Zhang,[a,1] X. H. Cheng,[b] and M. Zhu[b]

[a] School of Civil and Resource Engineering, University of Science and Technology Beijing, Beijing, China

[b] Department of Civil Engineering, Tsinghua University, Beijing, China

[1] shuang_you@163.com

Geothermal heat exchangers buried in diaphragm walls as an alternative of renewable energy sources can be quite competitive with shallow geothermal resources. The thermal response of a diaphragm wall embedded in the sand foundation under thermomechanical coupling conditions was followed in laboratory centrifuge tests. The model of exchanger tubes enclosed in the diaphragm wall embedded in the sand foundation accounts for lateral loading on the wall simulated by 1 and 50 g acceleration conditions in the centrifuge. Thermal loading, mechanical unloading, and thermo-mechanical coupling tests were carried out separately. The temperature, deformation, and soil pressure on the wall were monitored. The deformation and thermal stress along the cantilever wall were verified by numerical simulation. The thermal stress on the wall was revealed to be larger than the excavation-induced one. The maximum thermal stress was observed near the bottom of the wall. Though the wall was embedded in surrounding soil, heating caused accumulation of thermal stresses induced by temperature variations, which should be seriously considered in the heat exchanger design for cantilever walls of building structures.

Keywords: cantilever diaphragm wall, thermal stress, centrifuge model, deformation, dry sand.

Introduction. Shallow geothermal energy is an environmentally friendly form of renewable energy that can provide an alternative source of energy for heating/cooling buildings. The heat exchangers can be buried in piles, diaphragm walls and basement slabs. A fluid is circulated within the buried closed tubes to transport the heat stored in the soil to the heating/cooling system in the building above [1]. Xia et al. [2] investigated the heat transfer performance of geothermal heat exchangers installed in diaphragm walls in the Shanghai Museum of Natural History. Hamada et al. [3] embedded heat exchange pipes in friction piles for use in air-conditioning systems in offices and other civil buildings in Japan. Laloui et al. [4] conducted an in situ test of a heat exchanger pile under actual conditions at the Swiss Federal Institute of Technology in Lausanne. Stewart and McCartney [5] used a centrifuge model to investigate the mechanical behavior of an end-bearing pile subjected to cyclic heating. Goode et al. [6] used centrifuge models to investigate how thermal influenced the ultimate capacity of piles embedded in dry medium dense sand. Centrifuge models were also used to assess energy piles subjected to heating and cooling cycles in clay [7] and the heating effects of piles embedded in saturated sand [8], they found that shaft resistance of a pile increased as the temperature increasing, and toe resistance increased more rapidly than shaft resistance due to a larger downward expansion of the pile at higher temperature increment. The current understanding of thermomechanical (TM) interaction between wall and soil under elevated temperatures is still quite limited. Due to field studies are expensive and complicate, centrifuge modeling was used to study the TM coupling process. This approach provides a better understanding of the geotechnical design for safety control. In this study, the exchanger tubes enclosed in a diaphragm wall (Fig. 1) are designed and carried out in a dry sand foundation. The major

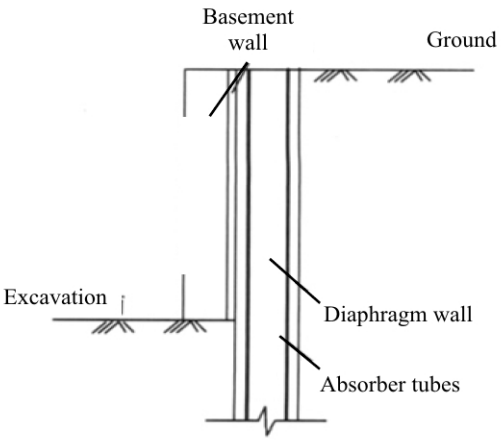

Fig. 1. Skeleton of the geothermal heat exchanger embedded in a cantilevered diaphragm wall.

objectives are to investigate thermal response of cantilevered diagram wall in TM coupling conditions. Moreover, related TM interaction between wall and soil under heating condition was also studied.

1. **Test Models and Procedure**.

1.1. ***Centrifuge Modeling***. To physically model the heat exchange in the diaphragm wall embedded in sand, a $1/N$ sized model of the prototype diaphragm wall was placed in a centrifuge and the heat diffusion processes were accelerated N^2 times compared with those in the field because the heat transfer rates were N times faster under $N-g$ conditions. The other relevant scaling laws are summarized in Table 1.

Table 1

Relevant Scaling Ratio ([9, 10])

Parameter	Model–prototype ratio	Parameter	Model–prototype ratio
Length	$1/N$	Strain	1
Temperature	1	Energy density	1
Density	1	Energy	$1/N^3$
Mass	$1/N^3$	Stress	1
Acceleration	N	Force	$1/N^2$
Velocity	1	Heat diffusion	$1/N^2$
Displacement	$1/N$		

1.2. ***Model Box Setup***. The geo-centrifuge at Tsinghua University has a maximum acceleration of 250*g*, a maximum load of 50*g*-ton, an effective radius of 2 m, a $0.8\times0.7\times0.6$ m nacelle, and a $0.6\times0.2\times0.55$ m model casing (Fig. 2). To simulate the thermal response of the diaphragm wall in the sand foundation in TM coupling conditions, all of the tests were performed under 50*g*. The cantilevered diaphragm wall was made of copper, and was 30 cm high, 20 cm wide, and 1.4 cm thick (the prototype was $15\times10\times0.7$ m). The excavation depth was 10 cm, which corresponded to a 5 m deep prototype excavation. A semiconductor chilling plate ($40\times40\times3.9$ mm) was used to heat the wall from the ambient temperature to around 50°C. The model was wrapped in foam plastic for thermal insulation.

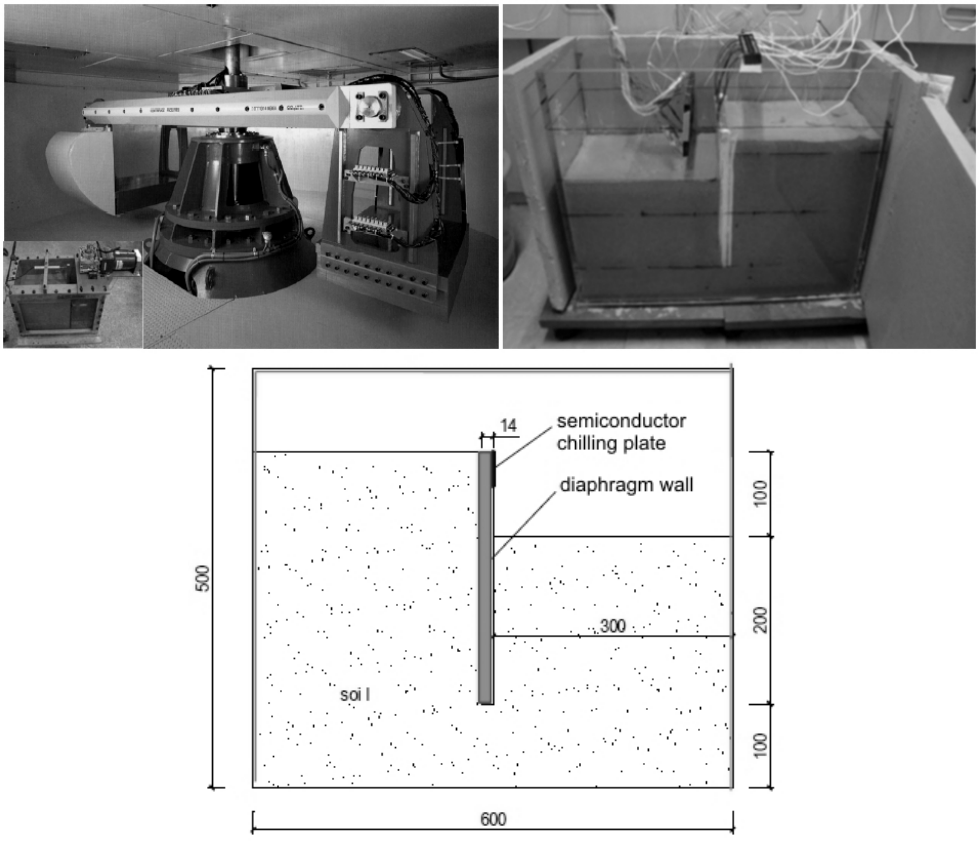

Fig. 2. Geotechnical centrifuge and model casing.

1.3. ***Measurements***. Six strain foils were affixed to the middle of the wall at depths of 10, 15, and 20 cm to monitor the vertical deformation of the wall. Soil pressure sensors were situated on both sides of the wall at depths of 10 and 20 cm to monitor the soil pressure. Twelve thermocouple temperature sensors were used to monitor the temperature distribution in the model, and one was used to monitor the ambient temperature. Six sensors were installed on each side of the wall (Fig. 3). A camera was used to monitor the movement of the soil.

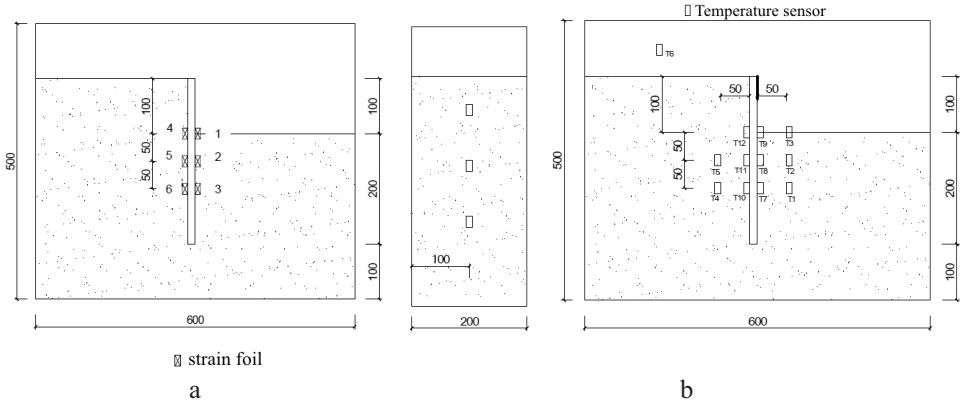

Fig. 3. Arrangement of the gauges in the testing model: (a) strain foil, (b) temperature sensor.

1.4. ***Testing Program***. Copper model energy cantilever tests with different temperatures and loading sequences were carried out in dry medium sand. The test program is summarized in Table 2. (i) Sensor calibration measurements were conducted under a 1*g* gravity field and an ambient temperature of 28℃ (summer in Beijing), and the results were used as a reference. (ii) A thermal coupling test was conducted under 50*g* with no excavation and the wall was heated to 50℃ to analyze the thermal effect on the soil pressure, with the thermal loading denoted as *t*. (iii) Mechanical tests were conducted under 50*g* with the wall excavated and a constant ambient temperature of around 28℃ to determine the influence of mechanical unloading on the mechanism of the wall, with the mechanical loading denoted as *m*. (iv) Finally, TM tests were conducted under 50*g* with the wall excavated on one side and heated to 50℃ to achieve a TM coupled field (denoted as *tm*). Overall, the tests aimed to simulate the geothermal energy circulating in the absorber tubes enclosed in the diaphragm wall embedded in the sand.

Table 2

Test Program

Test	Gravity field	Temperature (℃)	Loading sequence
i	*g*	28	none
ii	50*g*	50	*t*
iii	50*g*	28	*m*
iv	50*g*	50	*tm*

2. **Interpretation of the Test Results**.

2.1. ***Thermal Loading Simulations under 50g***. The centrifuge tests were performed at 50*g*, and the scaling relationships are listed in Table 1. As shown in Fig. 4, the temperature close to the wall drops quickly. In contrast, due to the heat transfer, the temperature of the soil (50 cm distance) slightly increases.

The unacceptably high strain on the wall might have been induced by the large expansion of the copper, which had a thermal expansion coefficient ($18.9 \cdot 10^{-6}\ ^\circ C^{-1}$), twice that of concrete ($9 \cdot 10^{-6}\ ^\circ C^{-1}$).The strain shows a downtrend as the temperature decreases (Fig. 5).

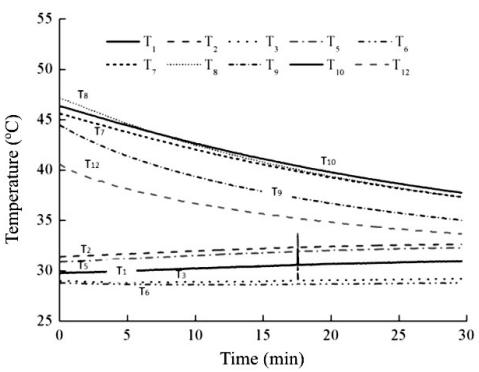

Fig. 4

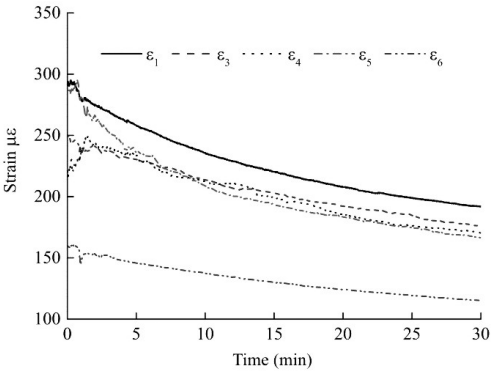

Fig. 5

Fig. 4. Temperature distribution along the wall with the time.
Fig. 5. Strain distribution along the wall with the time.

Figure 6 shows the increased stress induced by the heating of the wall and the average thermal stresses at the depths of 100 and 200 mm. Overall, the thermal stress increased with the depth and the stress recovered as the temperature decreased closer to the wall (Fig. 6). *Note*: tensile stress is defined as positive, compressive stress as negative.

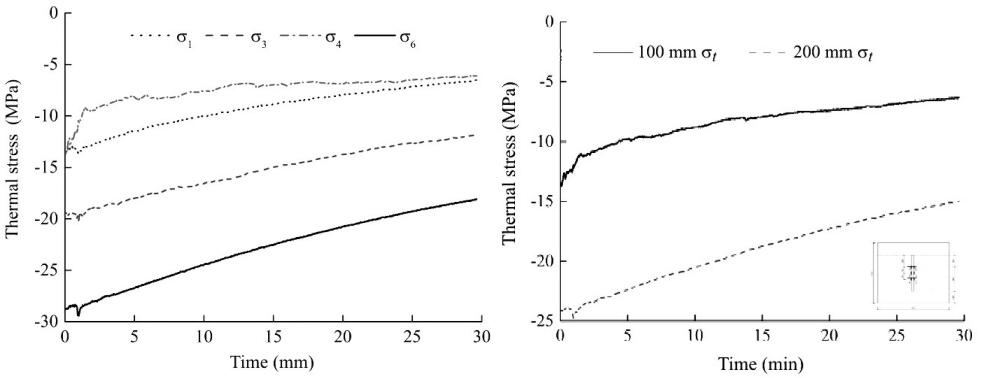

Fig. 6. Thermal stress distribution along the wall with the time.

2.2. ***Mechanical Unloading Simulation under 50g***. Under the constant ambient temperature of about 28℃ (Fig. 7), the strain changed smoothly due to the mechanical unloading (Fig. 8). Compressive strain was observed at points *3* and *6*, which were constrained by the soil.

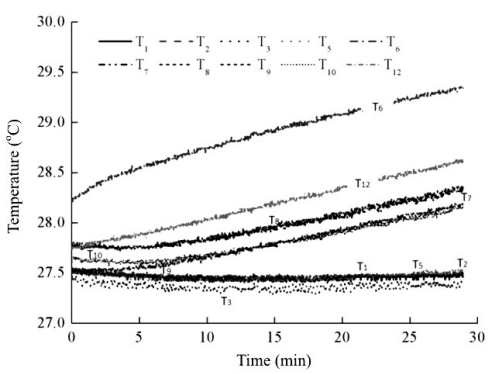

Fig. 7

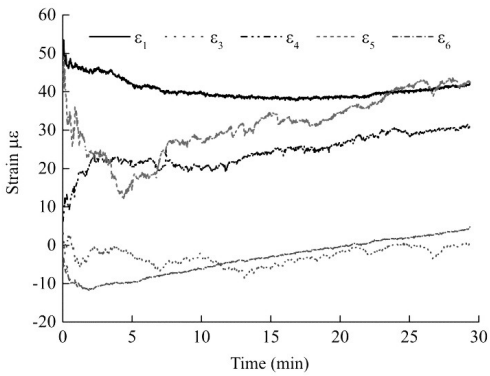

Fig. 8

Fig. 7. Temperature distribution along the wall with the time.
Fig. 8. Strain distribution along the wall with the time.

The increased stress induced by the excavation and the average stress at the depths of 100 and 200 mm are shown in Fig. 9. Compressive stress could be observed at the bottom of the wall and there was a greater distribution of stress on the excavated side than on the reverse face. *Note*: tensile stress is defined as positive, compressive stress as negative.

2.3. ***TM Coupling Simulation under 50g***. After the wall was heated to 50℃ and a steady temperature was attained, the heating instrument was disassembled. During the test, the temperature dropped quickly close to the wall, but increased slightly in the soil (50 cm from the wall), as is shown in Fig. 10.

Figure 11 shows that the strain decreased with the depth, while strain on the excavated side of the wall was higher than that in the corresponding point of its reverse side.

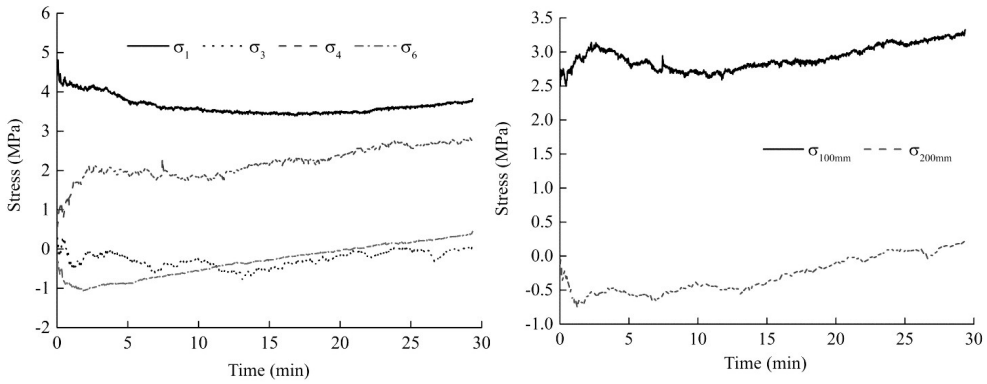

Fig. 9. Thermal stress distribution along the wall with the time.

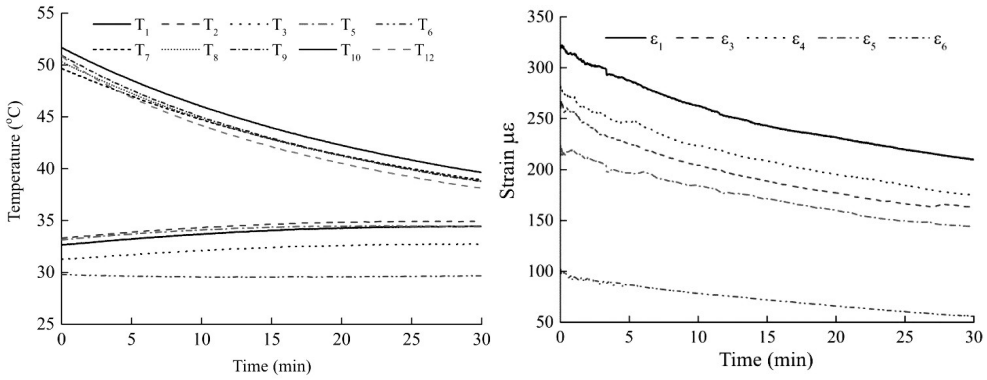

Fig. 10 Fig. 11

Fig. 10. Temperature distribution along the wall with the time.
Fig. 11. Strain distribution along the wall with the time.

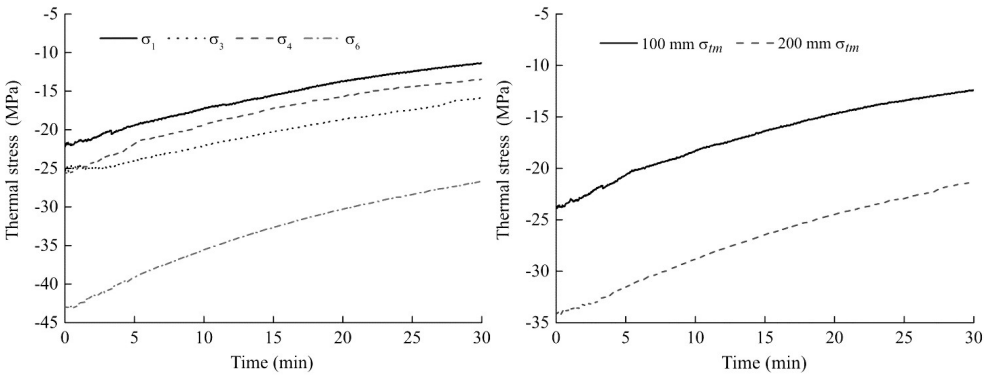

Fig. 12. Thermal stress distribution along the wall with the time.

Unacceptably high levels of strain were induced by the difference between the thermal expansion of copper ($18.9 \cdot 10^{-6}\ ^\circ C^{-1}$) and that of the concrete ($9 \cdot 10^{-6}\ ^\circ C^{-1}$). During the test (30 min), the strain recovered as the temperature decreased (Fig. 11).

Figure 12 shows the increases in thermal stress and the average thermal stresses at the depths of 100 and 200 mm under the TM coupling conditions. The thermal loading had a distinct effect on the distribution of the increases in stress. However, the stress recovered as

the temperature decreases (Fig. 12). *Note*: tensile stress is defined as positive, compressive stress as negative.

2.4. ***Comparison***. Comparison of the average stress distributions on the wall at the depths of 100 and 200 mm shows that the stress induced by the thermal transfer in the wall was greater than the excavation-induced stress (Fig. 13). The thermal expansion coefficient of copper ($18.9 \cdot 10^{-6}\ ^\circ C^{-1}$) was twice as large as that of concrete ($9 \cdot 10^{-6}\ ^\circ C^{-1}$), which might have caused the unacceptably high stress in the wall.

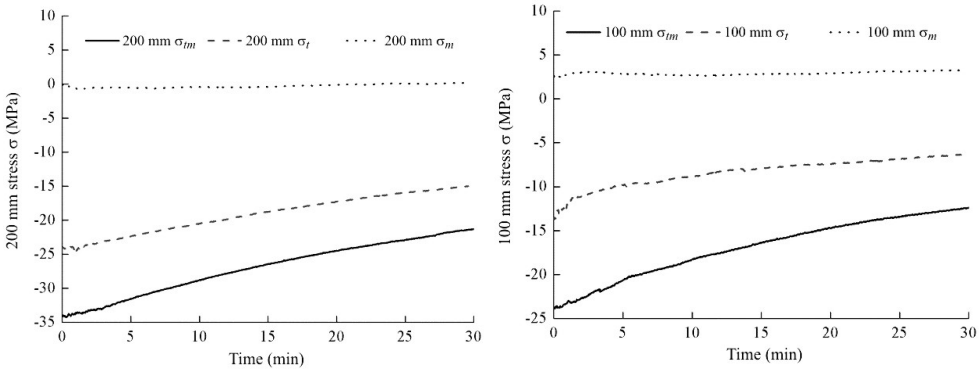

Fig. 13. Comparison of the thermal stress distributions in the wall at depths of 100 and 200 mm with the time.

Conclusions. In this study, centrifuge tests were performed on four models to investigate the thermal-excavation coupling mechanism of a cantilevered wall embedded in sand. The preliminary experimental tests show that the thermal stress in the wall was greater than the excavation-induced stress. The thermal stress was not uniformly distributed in the wall, with the maximum values observed near the bottom of the wall. The thermal stress was affected by the increased temperature in the wall and the constraining effects of the surrounding soil.

Acknowledgments. The authors are grateful for the funding provided by the National Nature Science Foundation of China (51774021), and the 'Geo-energy systems simulator: from building scale to city scale' of the Low Carbon Energy University Alliance of Tsinghua–Cambridge University–MIT LCEUA (20123010002). The first author gratefully acknowledges the financial support from China Scholarship Council (201706465003).

1. H. Brandl, "Energy foundations and other thermo-active ground structures," *Geotechnique*, **56**, No. 2, 81–122 (2006).
2. C. C. Xia, M. Sun, G. Z. Zhang, et al., "Experimental study on geothermal heat exchangers buried in diaphragm walls," *Energ. Buildings*, **52**, 50–55 (2012).
3. Y. Hamada, H. Saitoh, M. Nakamura, et al., "Field performance of an energy pile system for space heating," *Energ. Buildings*, **39**, No. 5, 517–524 (2007).
4. L. Laloui, M. Moreni, and L. Vulliet, "Comportement d'un pieu bi-fonction, fondation et échangeur de chaleur," *Rev. Can. Geotechnique*, **40**, 388–402 (2003).
5. M. A. Stewart and J. S. McCartney, "Centrifuge modeling of soil-structure interaction in energy foundations," *J. Geotech. Geoenviron.*, 140, No. 4, 04013044 (2014), doi: 10.1061/(ASCE)GT.1943-5606.0001061.
6. J. C. Goode III, M. Zhang, and J. S. McCartney, "Centrifuge modelling of energy foundations in sand," in: C. Gaudin and D. White (Eds.), *Physical Modelling in Geotechnics* (Proc. of the 8th Int. Conf. on Physical Modelling in Geotechnics, January 14–17, 2014, Perth, Australia), CRC Press (2014), pp. 729–735.

7. C. W. W. Ng, C. Shi, A. Gunawan, and L. Laluoi, "Centrifuge modelling of energy piles subjected to heating and cooling cycles in clay," *Geotech. Lett.*, **4**, No. 4, 310–316 (2014).
8. C. W. W. Ng, C. Shi, A. Gunawan, et al., "Centrifuge modelling of heating effects on energy pile performance in saturated sand," *Can. Geotech. J.*, **52**, No. 8, 1045–1057 (2015).
9. C. Savvidou, "Centrifuge modelling of heat transfer in soil," in: J.-F. Corté (Ed.), *Centrifuge 88* (Proc. of the Int. Conf. on *Geotechnical Centrifuge Modelling*, April 25–27, 1988, Paris), Balkema, Rotterdam (1988), pp. 583–591.
10. R. N. Taylor, *Geotechnical Centrifuge Technology*, CRC Press, London (2004).

Received 15. 03. 2018